NOTES AND CORRESPONDENCE

Characterizing Warm-ENSO Variability in the Equatorial Pacific: An OLR Perspective*,+

A. M. CHIODI

Joint Institute for the Study of the Atmosphere and Ocean, University of Washington, Seattle, Washington

D. E. HARRISON

Joint Institute for the Study of the Atmosphere and Ocean, University of Washington, and NOAA/Pacific Marine Environmental Laboratory, Seattle, Washington

(Manuscript received 13 January 2009, in final form 14 November 2009)

ABSTRACT

It is shown that space–time smoothed outgoing longwave radiation (OLR) indices of equatorial Pacific seasonal variability can give an interestingly different perspective on El Niño than is obtained from sea surface temperature (SST) indices or the Southern Oscillation index (SOI). In particular, the index defined by averaging over an eastern-central region exhibits strong event like character—more so than in any other El Niño–Southern Oscillation (ENSO) warm-phase index known to the authors. Although the historical record for OLR is much shorter than for SST or SOI, OLR offers a direct connection to anomalous atmospheric heating. It is suggested that the years identified as events by this OLR index deserve particular recognition; and it is noteworthy that they all meet the criteria for ''El Niño'' years. Other years, whose warm-ENSO status differs depending upon the index favored, are not particularly distinctive from an OLR perspective, and a case could be made that either the other years do not deserve special classification or that they should be identified as different from the OLR-distinguished El Niño years.

1. Introduction

The El Niño–Southern Oscillation phenomenon has become familiar around the world because substantial weather anomalies often occur during periods of extreme ''ENSO state.'' The warm and cold phases of ENSO—generally referred to as El Niño and La Niña, respectively—often bring anomalous regional seasonal rainfall and temperatures. Lists of years of extreme ENSO conditions have been composited, and multimonth life cycles of ''El Niño events'' and ''La Niña events,'' as well as associated seasonal weather anomalies, have been constructed and evaluated for the robustness of the characteristic marine surface and seasonal weather anomalies (see Ropelewski and Halpert 1987, 1996; Trenberth and Caron 2000; Harrison and Larkin 1998; Smith et al. 1999). Such composites provide a statistical basis for seasonal weather forecasting in the affected regions, if the statistical linkages are sufficiently strong (Leetmaa et al. 2001). The dynamical basis for such relationships is based on the fact that extremes of ENSO involve substantially anomalous patterns of deep tropical convection and, hence, of large-scale anomalous atmospheric forcing, which can be expected to drive both tropical and extratropical atmospheric circulation anomalies.

ENSO indices based on marine surface variability have been the most widely used. Seminal studies determined El Niño events based on SST variability along the Peruvian coast and along common shipping lanes in the far eastern tropical Pacific (Wyrtki 1975; Rasmusson

* National Oceanic and Atmospheric Administration/Pacific Marine Environmental Laboratory Publication Number 3205.

+ University of Washington's Joint Institute for the Study of the Atmosphere and Ocean Contribution Number 1511.

Corresponding author address: A. M. Chiodi, NOAA/Pacific Marine Environmental Laboratory, 7600 Sand Point Way NE, Box 357941, Seattle, WA 98115.
E-mail: andy.chiodi@noaa.gov

DOI: 10.1175/2009JCLI3030.1

and Carpenter 1982). Currently, Niño-3, -3.4 and -4 SST anomaly indices, representing averages over particular regions of the central tropical Pacific, are in wide use. Of these, Niño-3.4 has been identified as optimum based on a number of criteria (Barnston et al. 1997; Trenberth 1997). The Southern Oscillation index (SOI) representing the sea level pressure (SLP) difference between the islands of Tahiti and Darwin is also in wide use. Multivariate indices, such as the Bjerknes ENSO index (BEI; see Harrison and Larkin 1998) and the multivariate ENSO index (Wolter and Timlin 1998), have also been proposed but have not gained wide acceptance. ENSO indices do not always vary consistently with each other [see Deser and Wallace (1987) for examples involving SLP and SST indices] and, thus, the characteristics of ENSO are different depending upon the index selected. Some ENSO indices have rather continuous, Gaussian like probability distributions. Others are more ''event like,'' with significant departures from Gaussian-type behavior. Thus, some indices (event like) are more consistent than others (Gaussian like) with the traditional practice of classifying distinct ''ENSO event'' years.

Recently, Larkin and Harrison (2005a,b) have suggested that there exists a need to distinguish some years with warm tropical Pacific SST anomalies (SSTA) from others based on the fact that the composite-averaged global seasonal weather anomalies depend on the spatial distribution of the SSTA. Particularly, years with warm Niño-3.4 anomaly that have not been commonly agreed upon as El Niño years were shown, in an average sense, to have different seasonal weather anomalies than those more commonly agreed upon.

We provide a view of recent warm-ENSO variability using outgoing longwave radiation (OLR) measurements, which have been available reliably from satellite measurements since about 1979. The tropical Pacific undergoes large intraseasonal and interannual variations in deep atmospheric convection (Trenberth et al. 1998). By suitable averaging of OLR over space and time, it is possible to filter out the intraseasonal variability. In the tropics, OLR variability is a good proxy for the deep atmospheric convection conditions that generate atmospheric heating anomalies and force local and remote atmospheric circulation anomalies [see Lau et al. (1997); Garreaud and Wallace (1997, 1998); see also Arkin and Meisner (1987) for a related cloud fraction index]. Chelliah and Arkin (1992, hereafter CA92) have previously recommended a date-line-centered ''OLR ENSO index.'' Curtis and Adler (2000) also previously suggested the ''ENSO precipitation index'' (ESPI), based on a measure of the zonal precipitation gradient between the tropical Pacific and Maritime Continent regions. Analysis herein of the covariability of OLR and 500-mb geopotential height anomaly (described later) identifies a different region than recommended by CA92 as predominantly important to tropically driven global atmospheric circulation anomalies. Later, a view of recent warm-ENSO variability is constructed based on OLR behavior in this [eastern-central Pacific (ECP)] region and is compared to that offered by some widely used ENSO indices and the indices suggested by CA92 and Curtis and Adler (2000).

It is shown that a distinct type of OLR behavior was observed over the eastern-central Pacific (defined broadly here as the region 5°S–5°N, 170°–100°W) in four satellite-era years commonly agreed upon as ''El Niño'' (1982/83, 1986/87, 1991/92, and 1997/98). In these years, OLR values typical of the convectively active western Pacific were observed in the eastern-central Pacific, in a broad region-averaged sense. The other years in this period are not particularly distinct from an OLR perspective.

2. Data

We use monthly averages of the daily ''interpolated OLR'' data provided by the National Oceanic and Atmospheric Administration's Office of Oceanic Atmospheric Research/Earth System Research Library's Physical Sciences Division (NOAA/OAR/ESRL PSD), Boulder, Colorado, from their Web site (available online at http://www.cdc.noaa.gov). This is a satellite-derived product available on a 2.5° × 2.5° grid. Details of the interpolation technique are described in Liebmann and Smith (1996). Here, anomalies are determined from monthly average climatology (base period 1979–2007), though we also consider absolute monthly OLR values, since these offer a more direct connection to anomalous atmospheric heating.

We also consider various SSTA-based ENSO indices (same base period as OLR for consistency), determined from the NOAA Extended Reconstructed Sea Surface Temperature (ERSST) dataset (version 3, available online at http://www.cdc.noaa.gov/cdc/data.noaa.ersst.html; Smith et al. 2007). Conventional spatial averaging procedures were used to obtain the Niño-4, Niño-3.4, Niño-3 (5°S–5°N, 160°E–150°W; 5°S–5°N, 170°–120°W; and 5°S–5°N, 150°–90°W, respectively) and Niño-1+2 indices (10°S–0°, 90°–80°W). A 3-month running-average filter was applied to each of these indices, consistent with common practice and the current NOAA Climate Prediction Center Niño 3.4–based ''oceanic Niño index'' definition. Interested readers are referred to Chiodi and Harrison (2008) for results of similar analyses using monthly average SSTA. Results consistent with those discussed here (but not shown) can also be obtained using Met Office Hadley Centre Sea Ice and Sea Surface

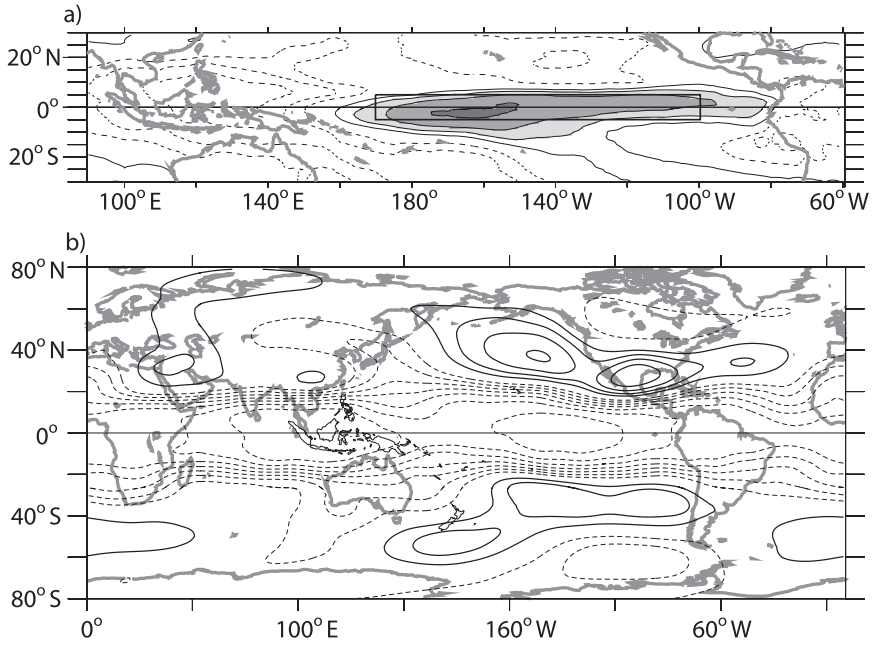

FIG. 1. (a) Dominant OLR pattern (i.e., homogeneous correlation map) from the joint SVD of OLR and 500-mb geopotential height anomaly. Correlation contours every 0.2 with 0 contour omitted. Box shows the 5°S–5°N averaging region that results in the closest agreement between time series based on OLR-side temporal SVD results and simple spatial average of OLR anomaly. (b) Dominant geopotential height anomaly pattern (heterogeneous correlation map). Contours every 0.1 with 0 omitted.

Temperature dataset (HadISST) version 1 data (data available online at http://hadobs.metoffice.com/hadisst/).

Monthly averaged values of the mean sea level pressure at Darwin and Tahiti were obtained from the Australian Bureau of Meteorology. These data are available online (at http://www.bom.gov.au/climate). The definition for SOI used here is the one suggested as optimum for the consideration of interannual anomalies by Trenberth (1984). In this case, a weighted, 13-month running-average filter is used to filter out intraseasonal and higher-frequency atmospheric variability (e.g., Madden–Julian oscillation) that occurs regardless of ENSO state. We note, however, that 30- or 90-day running averages are in common use for operational identification purposes.

Monthly values of the ESPI were obtained from the National Aeronautics and Space Administration's (NASA) Goddard Space Flight Center (data available online at http://precip.gsfc.nasa.gov/).

3. Results

a. Identifying an OLR index region

To statistically determine the patterns of OLR variability that are most strongly linked to broad-scale atmospheric circulation anomalies, we examine the joint singular value decomposition (SVD) of OLR and global 500-mb geopotential height ($z500$) anomaly. In this case, the OLR region considered is bounded by 30°S and 30°N, but all latitudes are considered (this was also done in the analyses described by CA92, which considered only OLR variability). Results using normalized monthly averages of OLR and $z500$ anomaly are discussed here (normalization accomplished here by dividing by the standard deviation at each grid point), though qualitatively similar results are obtained using 3-month running averages, and/or nonnormalized data (not shown). Readers are referred to Bretherton et al. (1992) for a more thorough discussion of the properties of SVD analysis than is given here.

The dominant SVD pattern of OLR anomaly (OLRA) covariation shows a broad maximum spanning the central equatorial Pacific [Fig. 1a; as is now customary, we present the ''covarying part'' of the OLR anomaly by showing the correlation between the OLR-side SVD time-expansion coefficients and the monthly OLR anomaly, called the ''homogeneous correlation map'' by Bretherton et al. (1992)]. In this case, peak values are seen in the region bounded by the date line and about 150°W, though substantial correlation also extends to the far eastern equatorial Pacific. The temporal variability (OLR-side SVD expansion coefficients) of this OLR anomaly pattern

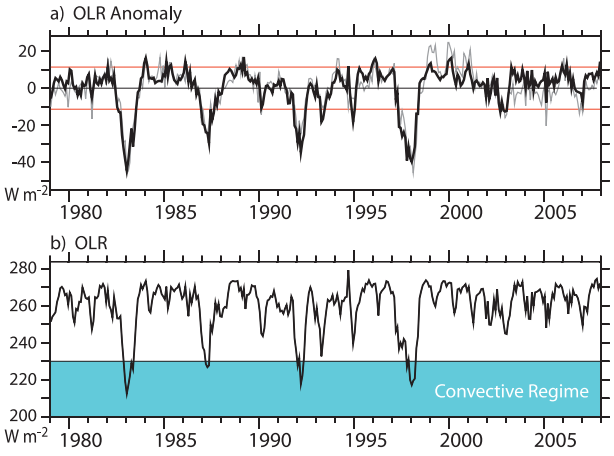

FIG. 2. (a) Area-average monthly OLR anomaly (black curve, 5°S–5°N, 170°E–100°W) and the OLR-side temporal SVD results (i.e., OLR expansion coefficients) (gray curve, scaled to have the same standard deviation as the area average); thin red straight lines at $\pm 1\sigma$. (b) Absolute monthly OLR values averaged over same region as shown in (b). Light blue shading for values indicative of deep convection.

is well reproduced by the index formed by averaging the OLR anomaly over the region bounded by 5°S, 5°N and 170°E, 100°W (cf. black and gray curves in Fig. 2). In this case, 170°E and 100°W were the round-numbered bounds found to give the highest correlation with the SVD results. The bounds 5°S and 5°N are also used by the CA92-recommended index and the commonly referred to SSTA-based ENSO indices (discussed later).

In this case, focusing on the first SVD mode appears justified since it explains 56% of the (squared) covariance (Bretherton et al. 1992), whereas the second and third modes (not shown for brevity) explain only 7% and 6%, respectively. Also, these two lesser modes were found upon inspection to resemble some lesser modes discussed previously in statistical examinations of OLR variability [specifically, CA92 modes 3 and 2 and Waliser and Zhou (1997) modes 4 and 3], which were interpreted to primarily reflect aliasing effects caused in part by the need to rely on OLR measurements from different satellites over the study period, and by some OLR anomaly features that occur around the time of the largest first-mode events (e.g., 1982–83) but are not contained in the dominant mode.

b. *The eastern-central Pacific OLR perspective*

A distinct type of variability is seen in the index formed by averaging OLR anomaly over the broad ECP region highlighted by this joint SVD analysis (Fig. 2a). Most notably, the amplitudes and durations of the anomalies seen during the interannual periods of 1982/83, 1986/87, 1991/92, and 1997/98 rather unambiguously distinguish these events from the background OLR anomaly variability seen at other times.

Absolute ECP OLR values (Fig. 2b), which serve as a proxy for anomalous atmospheric heating, are most often (about 84% of the time) above 250 W m^{-2}, indicating that nonconvective conditions persist, in a regional and monthly average sense, in the ECP throughout most years (even though the western portion of the region considered here may see considerable localized convection). ECP OLR typically shows a strong seasonal cycle (see Fig. 2b), in which seasonal minima in the 250–260 W m^{-2} range are usually seen in the months of March or April and maxima, ranging from about 265–290 W m^{-2}, occur around September. Convective activity during the large events of 1982/83, 1986/87, 1991/92, and 1997/98, however, was quite different from this usual behavior. In these four events, ECP reached annual minima at different times of the year and at well below normal values, reaching levels more typical of the convectively active western Pacific. During these events, monthly averaged ECP OLR even crossed into the deep convective regime (OLR $<$ 230 W m^{-2}; see Garreaud and Wallace 1997, 1998) in a regionally averaged sense (see Fig. 2b).

It is notable that these four events are commonly agreed upon as warm-ENSO events, and that the areas under these four peaks are qualitatively consistent with the generally agreed upon relative sizes of recent warm-ENSO events (e.g., the 1982/83 and 1997/98 events are larger than the 1986/87 and 1991/92 events). Given the unusual size of these four events, a wide range of threshold values can be used to unambiguously distinguish these events from background variability. Thus, these four events can be clearly identified by visual inspection, and a case can be made that they represent significant events—both on a statistical (discussed in greater detail later) and phenomenological (OLR crossing to the convective regime) basis.

c. *Comparison with other ENSO indices*

Although there is significant agreement between the ECP OLR anomaly and Niño-3.4 SSTA indices (see Fig. 3b; Table 1), it is clear that the relationship is not a perfect match. There is general agreement among the relative sizes of the four largest events from each index, which roughly coincide with each other. It is clear, however, that there were several years with warm Niño-3.4 SSTA [~(0.5–2) standard deviations (σ) warmer than average] but nearly normal ECP OLR values (e.g., 1979/80, 1992/93, 1994/95, 2002/03, 2004/05 and 2006/07). Thus, while it is true that the four largest ECP-convection events occur during times of warm Niño-3.4 SSTA, the

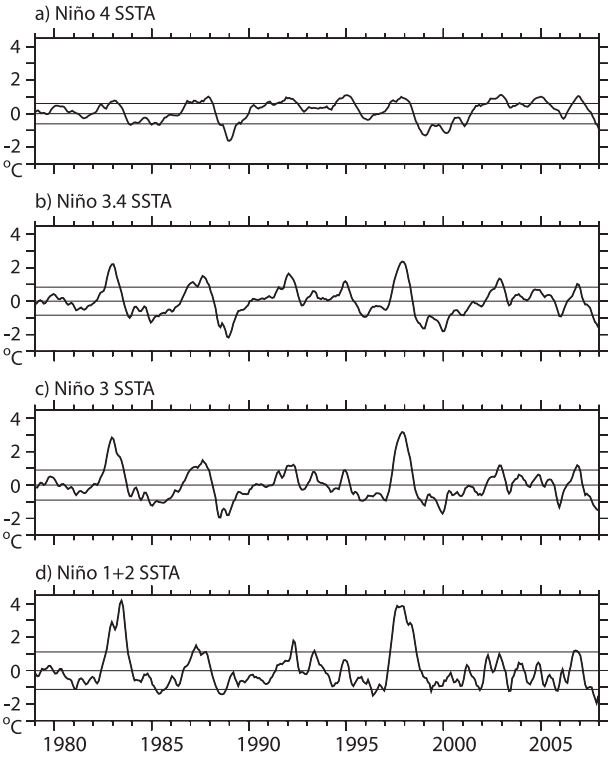

FIG. 3. SSTA averaged over the Niño-4, -3.4, -3, and -1+2 regions (see text for region bounds). A 3-month running-average filter has been applied in each case.

converse does not hold; warm Niño-3.4 SSTA does not necessarily lead to convection over the ECP. This suggests that warm Niño-3.4 SSTA is a necessary but insufficient condition for convection to reach the ECP.

The distributions of the amplitudes of the interannual anomalies seen in the ECP OLRA and Niño-3.4 SSTA indices have significantly different character, which can lead to different assessments of recent tropical Pacific variability, depending on the choice of index. There is significant separation between the peak amplitudes of each of the largest four ECP OLRA events and the observed background variability. Each of these four (negative) peak amplitudes exceeds the time series mean by 2.5σ, and the two largest have peak amplitudes in the $(3.75–4.0)\sigma$ range. The peak amplitude of the lesser of these four events (1986/87) is about 1σ greater than the next highest (seen in 1992/93), leaving a significant gap between the peak amplitudes of the four largest (negative anomaly) events, and the amplitudes of the other interannual anomalies, which are all within about 1.6σ of the overall time series mean. This feature makes the four largest events stand out from the other variability resolved by this index.

The picture from Niño-3.4 SSTA is rather different. Using 1σ as a rough threshold value, the number of events

TABLE 1. Correlation of ECP OLR index and other ENSO indices in the period 1979–2007. Values shown are for monthly averaged indices. In the SOI case, the value in parentheses is for the smoothed SOI.

Niño-4	Niño-3.4	Niño-3	Niño-1+2	SOI	CA92	ESPI
−0.55	−0.79	−0.84	−0.78	0.66 (0.76)	0.77	−0.81

that can be unambiguously distinguished from Niño-3.4 SSTA is two: the events of 1982/83 and 1997/98, which peak in the $(2.5–3)\sigma$ range. This leaves the commonly agreed upon warm-ENSO events of 1991/92 and 1986/87 in the mix of four other single-peak events within 1σ of the 1991/92 event peak (1994/95, 2002/03, 2004/05, and 2006/07) in addition to, possibly, events in 1987/88 and 1990/91, depending on annum chosen (1987/88 is given event status more commonly than 1990/91). The peaks of these anomalies are not very well separated in amplitude from several other interannual warm anomalies that peak above 0.5σ (e.g., 1979/80, 1992/93, 2003/04, and 2005/06). Thus, we find that the number of warm events determinable from Niño-3.4 SSTA alone depends rather precisely on the threshold value used.

Looking farther east, we see an increase in relative separation between the two highest SSTA peaks (in 1982/83 and 1997/98) and the background variability resolved in the Niño-3 and Niño-1+2 indices (more so for Niño-1+2; cf. Figs. 3c and 4d), but the amplitudes of the secondary peaks remain rather continuously distributed and relatively close to the mean. From this perspective, classifying anomalies using Niño-3 or Niño-1+2 is similar to using Niño-3.4, and these three SSTA-based indices relate similarly to OLR variability. A somewhat different type of SSTA behavior is seen in the western Pacific Niño-4 region, in that the peaks of the 1982/83 and 1997/98 anomalies do not stand out especially from others, and the amplitudes of the warm-anomaly peaks do no rise much above 1σ (Fig. 3a).

SOI is significantly correlated with the other time series considered here (Fig. 4a; Table 1) though discrepancies are apparent and can lead to interpretations of interannual anomalies different from those of SSTA, as has been discussed in previous work (Deser and Wallace 1987). Nonetheless, some of the lowest minima in SOI are seen at the times of the four largest eastern Pacific OLR events discussed earlier, confirming these as conventional warm-ENSO years (i.e., both El Niño and ''Southern Oscillation'' years). In SOI, however, these four events do not stand out significantly from several other troughs with roughly the same amplitude (e.g., 1992/93, 1994/95, 2002/03, and 2004/05). Here we have considered low-pass-filtered SOI to highlight interannual variability (as recommended by Trenberth 1984). The results of the

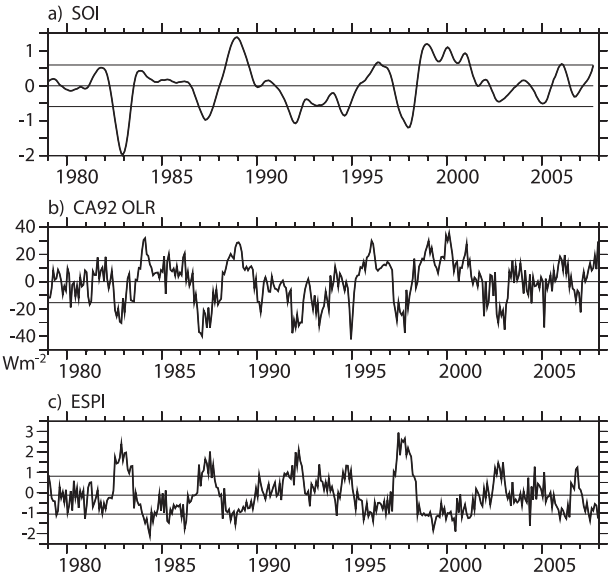

FIG. 4. (a) The SOI. (b) The CA92 index. (c) The ESPI suggested by Curtis and Adler (2000). Please note that the weighted 13-month running-average filter suggested by Trenberth (1984) has been applied to SOI.

analysis described earlier, however, are qualitatively similar for monthly average SOI values (see Chiodi and Harrison 2008).

The ESPI is determined from a measure of the difference in precipitation rate between the Maritime Continent region and the central tropical Pacific, and it was designed to ''ensure a good relationship with SST and pressure-based indices'' (Curtis and Adler 2000). It is also highly correlated with ECP OLRA, (see Fig. 4c; Table 1), though substantial differences in the character of these two indices are apparent. Whereas the peaks of the four largest convective-type interannual anomalies are separated from the others by at least 1σ in ECP OLRA, none of the interannual peaks in the ESPI are distinguished by this amount; the largest separation (0.6σ) occurs between the amplitudes of the (larger) 1997/98 and 1982/83 anomalies. The ESPI also appears to be more affected than ECP OLR by intraseasonal variability. Curtis and Adler also suggested a related precipitation-based El Niño index (EI). The relationship between EI (not shown for brevity) and ECP OLR is qualitatively similar to that discussed earlier. After the two largest EI peaks (separated from the third largest by 0.8σ), there is only a rather small amount of separation between the amplitudes of subsequent interannual anomalies; the amplitudes of the next five highest-ranking anomalies are spread within the gap of about 0.5σ that separates the third and eighth largest anomalies.

The convective behavior of the date-line-centered CA92 OLR-based index (5°S–5°N, 160°E–160°W) is similar in some respects to that of the eastern Pacific, but it shows some important differences on interannual time scales (cf. Figs. 2a and 4b). CA92 and ECP OLRA are positively correlated, and convective events (troughs) are seen in the CA92 index during times roughly coincident with the four largest eastern Pacific events. The relative sizes of the CA92 convective events, however, are different than those in the eastern Pacific. For example, the amplitudes attained during the 1986/87 and 1991/92 CA92 events are larger than those seen in 1997/98 and 1982/83. And an event not particularly distinguished by ECP OLRA (1994/95) attains the largest amplitude in the period considered. In addition to these, several other CA92 events with similar amplitude and duration were observed during years in which the eastern Pacific exhibited mostly normal behavior. Such CA92 anomalies were seen in some years with warm-event status based on some ENSO indices (e.g., 2002/03, 2004/05, and 2006/07) and others usually not considered to be warm events (e.g., 1992/93 and 1989/90). Unambiguously classifying event years based on the CA92 index is made difficult by the fact that amplitudes of interannual anomalies are rather continuously distributed (this is discussed more later).

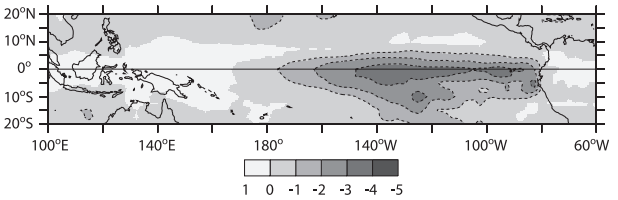

FIG. 5. Skew of monthly average OLR anomaly (period 1979–2007).

It is also notable that, whereas eastern Pacific OLR variability is dominated by convective events, CA92 index variability does not particularly favor anomalies of one sign or the other; positive anomaly (clear sky) events are nearly as large as negative anomaly (deep convection) events. This can be partially understood by considering the skew[1] of monthly averaged OLR anomaly in the tropical Pacific (Fig. 5), which shows that the CA92 index mixes regions of moderate (magnitude <1) negative and positive skew, whereas eastern-central Pacific OLR variability is distinguished by rather large (<-2) negative skew. Inspection has shown that indices qualitatively similar to the eastern Pacific average shown earlier (but more highly skewed) can be obtained by averaging OLR anomaly over subregions of the eastern equatorial Pacific

[1] Skew is a statistical measure of the relative strength of the tails of a distribution; that is, negatively (positively) skewed variables have relatively strong negative (positive) tails.

that include the skew minima seen in the eastern-central Pacific, centered near 135°W.

d. Index distributions

Visual inspection of the indices discussed earlier suggests that ECP OLR is more eventlike than some of the commonly used ENSO indices (e.g., Niño-3.4, SOI). To further examine this, the distributions of the indices discussed earlier are shown in Fig. 6. Here, 1σ-spaced bins are used, though results are qualitatively similar at $(0.25–2.0)\sigma$ spacing. For comparison, we show the 95% (upper bar) and 5% (lower bar) probability levels, as well as an expected value (middle bar), for a Gaussian-distributed variable with the same mean and σ as found in the observations. The probability levels were estimated by Monte Carlo methods (described in the appendix) and give a rough indication of whether the observed variability is consistent with Gaussian behavior; a variable that is consistent with Gaussian behavior cannot be said to be very eventlike [see Chiodi and Harrison (2008) for a discussion of the distributions of interannual anomaly amplitudes that can be expected from Gaussian-type behavior].

The distribution of monthly-mean values of eastern Pacific OLR anomaly is non-Gaussian in many respects (Fig. 6a). Three of the four negative-tail bins (-1, -2, -3, and $-4)\sigma$ contain values inconsistent with Gaussian-type behavior; the 1σ bin [bounds of $(0.5–1.5)\sigma$], which contains values either leading up to the four convective events or peaks of secondary anomalies, is significantly less populated than expected based on Gaussian behavior; the -2σ bin is consistent with a Gaussian-type behavior but is mainly composed of values in the growth–decline stages of the large events (17 of the 19 values, or about 90% of the values in this bin are large event growth–decline values; 2 values are peaks of secondary events); the -3σ and -4σ bins, which contain values only from the four large events, both contain more values than expected. Together, these features make the four large events stand out rather unambiguously from the secondary events.

A feature of this index that is particularly uncommon to Gaussian-type behavior is that it crosses the -3.5σ level on two occasions: during the events of 1982/83 and 1997/98. Since only about 0.046% of the area (two tailed) under a Gaussian distribution curve lies this far from the mean, the binomial distribution can be used to determine the probability (p_1) that this threshold would be exceeded 2 or more times by a Gaussian-distributed variable. Using values of degrees of freedom (DOF) per year from 1 to 3 (cf. estimation methods in Harrison and Larkin 1997; Leith 1973), p values for this feature range from 8.5×10^{-5} to 7.7×10^{-4}. Thus, the ''false discovery rate'' (FDR) methods discussed by Wilks (2006; $p_1 < p_{\mathrm{FDR}} = 8.3 \times 10^{-3}$, in this case at the 95% level) show that the ECP OLR index is significantly non-Gaussian, in an overall sense.

We have repeated the binning analysis discussed earlier for each of the other ENSO indices considered here. The notable result in the cases of the Niño-4, Niño-3.4, SOI, ESPI, and CA92 indices is that none of these indices show significant departures from Gaussian-type behavior; none of the bins shown in Figs. 6b–f contain values that exceed the $p = 0.05$ or $p = 0.95$ levels (upper and middle hash marks in Fig. 6). This is also the case for unfiltered monthly values of Niño-3.4 and SOI (not shown). Given this result, it is not surprising that the amplitudes of interannual anomalies seen in the index described earlier are rather closely ranked [see Chiodi and Harrison (2008) for the expected ranking of Gaussian-type events]; thus, ''events'' cannot be distinguished from ''nonevents'' in an unambiguous manner by consideration of these indices alone.

It is interesting to note, however, that the distribution of the more traditional, but currently less referred to, Niño-1+2 index shows significant departures from Gaussian-type behavior (this is true also for Niño-3 but to a lesser degree than Niño-1+2; cf. Figs. 6g and 6h). The Niño-1+2 index has more values near the mean and fewer moderately anomalous values than expected for a Gaussian-type variable (though not significantly so), and it has significantly more values in the positive (warm SSTA) tail. Thus, this more traditionally used index is more consistent than Niño-3.4 SSTA or SOI with the traditional practice of classifying distinct El Niño states (e.g., Wyrtki 1975; Rasmusson and Carpenter 1982).

We have confirmed that the results of this section are consistent with those obtained from the more commonly used Lilliefors test for normality (see Wilks 1995). For example, the ECP OLR index is determined to be significantly different from a Gaussian-distributed variable, whereas the behaviors of the Niño-4, Niño-3.4, SOI, ESPI, and CA92 indices cannot be said to be significantly different from Gaussian-type behavior, according to the Lilliefors test (test statistics and critical values are given in Table 2).

4. Discussion and conclusions

The perspective on recent warm-ENSO behavior offered by the eastern-central Pacific OLR index discussed here is differen from that offered by the most commonly used ENSO indices (e.g., SOI and Niño 3.4). This OLR

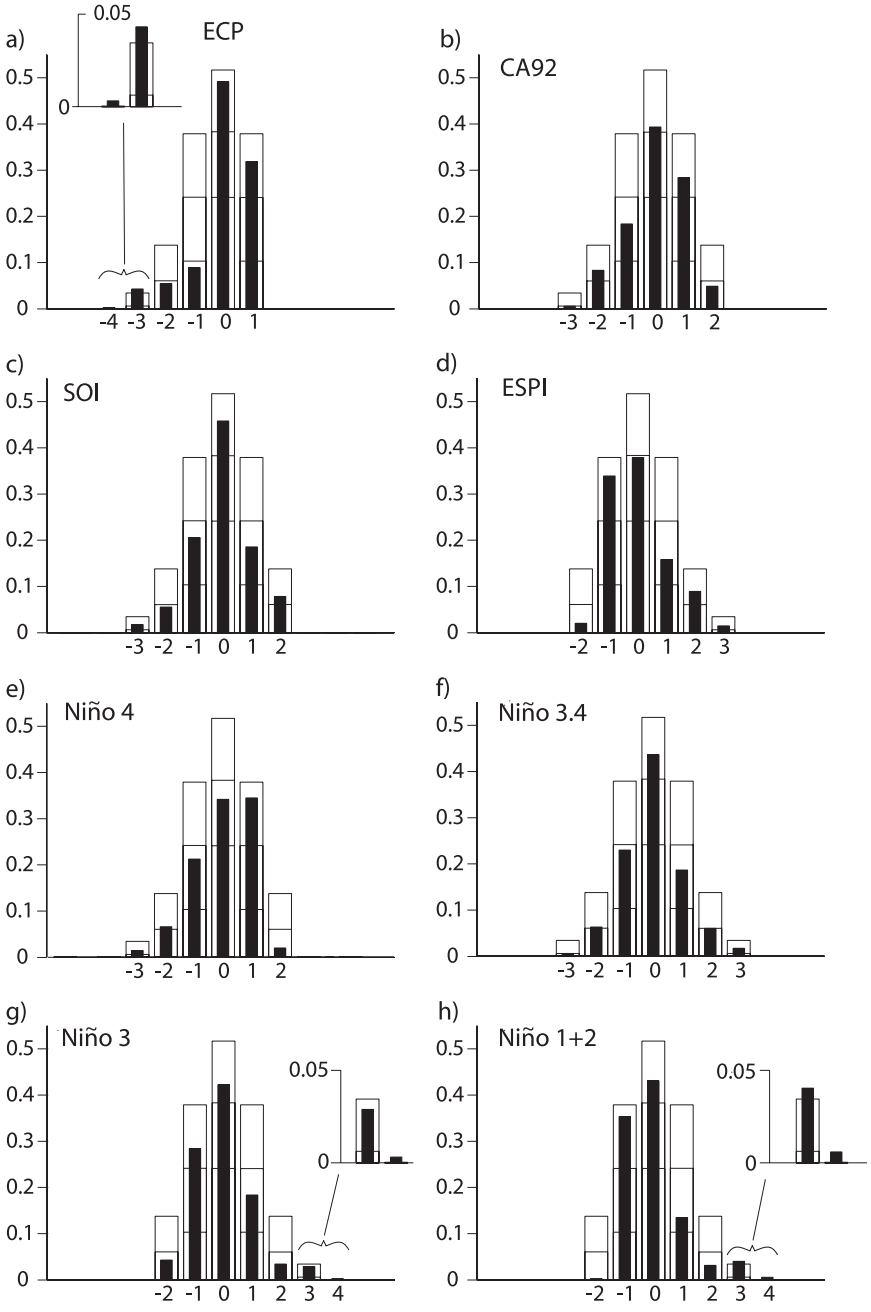

FIG. 6. Frequency distribution of monthly values of (a) ECP OLRA index, (b) CA92 OLRA index, (c) SOI, (d) ESPI, (e) Niño-4 SSTA, (f) Niño-3.4 SSTA, (g) Niño-3 SSTA, and (h) Niño-1+2 SSTA. Bin spacing is 1σ in each case (centered at . . . , −1, 0, 1, etc.). Upper and lower hash marks in each bin shows 0.95 and 0.05 probability levels for a Gaussian-distributed variable with equivalent mean and standard deviation. Temporal smoothing is consistent with the curves shown in Figs. 3 and 4; monthly averages for OLR and ESPI, 3-month running averages for SSTA, and Trenberth (1984)–type smoothing for SOI (results remain qualitatively similar using monthly average SSTA and SOI).

perspective rather unambiguously distinguishes four satellite-era (1979–2007) years commonly agreed upon as El Niño years: 1982/83, 1991/92, 1986/87, and 1997/98. The same cannot be said for the SSTA-based indices or SOI. In the case of the SSTA indices, two interannual time-scale events stand out from the rest: 1982/83 and 1997/98. While the ECP OLR–based index confirms that these two events are the largest in recent record

TABLE 2. Values of the Lilliefors test statistic (D), which tests for the maximum difference between the empirical and theoretical (Gaussian) cumulative distribution functions. Depending on the estimation method used (cf. Harrison and Larkin 1997; Leith 1973), the number of DOF in these time series (period 1979–2007) can range from 29 (one a year) to 87 (three a year). The Lilliefors 95% (99%) confidence level (Wilks 1995, Table 5.2) for $D_{87} = 0.0950$ (0.1105) and $D_{29} = 0.1470$ (0.1882). Thus, the ECP OLR index is significantly different from a Gaussian-type variable at the 99% level in even the strictest of these cases (fewest DOF). Whereas, with the exception of Niño-1+2, the hypotheses that the other indices considered have Gaussian distributions cannot be rejected at 95%, according to this test.

Index	ECP OLRA	Niño-1+2	Niño-3	Niño-4	SOI (filtered)	ESPI	Niño-3.4	CA92 OLRA
D	0.2174	0.1284	0.0834	0.0785	0.0746	0.0697	0.0627	0.0548

(consistent with the commonly agreed upon relative sizes of El Niño events), the more interesting question is, how many more events occurred in the satellite era? Since SOI and the SSTA-based indices show numerous other interannual anomalies that are not very well separated from each other or from background variability, we find it difficult to satisfactorily answer this question from SLP and SSTA information alone.

It is shown that the distribution of ECP OLR is significantly ''eventlike,'' whereas the most commonly used indices are shown to essentially behave like Gaussian-type variables. The use of an eventlike index, such as ECP OLR, is ideal for the type of compositing studies that have previously revealed useful information about the types of global seasonal weather anomalies that occur during periods of extreme ENSO state, and the mechanisms responsible (e.g., Rasmusson and Carpenter 1982; Ropelewski and Halpert 1987, 1996; Trenberth and Caron 2000; Harrison and Larkin 1998; Smith et al. 1999). We therefore suggest that using OLR information to determine the warm-ENSO state of the tropical Pacific is more consistent with the ongoing practice of operationally determining distinct warm-ENSO states than using the most commonly referred to indices.

It is notable that the ECP OLR–based index, derived from monthly rather than longer-term means, often gave an early enough indication of an oncoming event to be useful to midboreal-winter-and-later forecasting efforts. This index is therefore suitable for operational determination of warm-ENSO events. The SSTA-based definitions currently in place more often gave an earlier indication of an ensuing warm-ENSO event, although not all warm-SSTA conditions lead to distinctive convection conditions. We suggest that an operational system that uses OLR information to confirm event status, and other sources of information to determine event likelihood, may be optimal.

The ECP OLR perspective is also different from that offered by the ESPI and the OLR-based index suggested by CA92. In each case, different regions, each with a somewhat distinct type of variability, were used to determine the indices. Chelliah and Arkin focused on OLR variability around the date line, where OLR variance is highest, but peaks with amplitude and duration similar those seen in the events distinguished by ECP OLR can be seen in several other years, including some that have not been traditionally considered warm-ENSO years. We suggest that the occurrence of deep convection in this region can be considered an aspect of, but not exclusive to, the El Niño phenomenon. In the ESPI case, precipitation anomalies in the Maritime Continent region are considered in addition to anomalies in a region similar to the one mainly considered here. In preliminary studies that considered OLRA averaged over multiple 30° longitude by 10° latitude-spaced boxes spanning the Pacific, visual inspection failed to reveal distinct OLR variability on interannual time scales in the western Pacific and Maritime Continent regions. We suspect that, not withstanding the moving-average method used to determine the ESPI (Curtis and Adler 2000), the inclusion of information from this region can explain much of the difference between the ESPI and ECP OLRA index.

Recently, Larkin and Harrison (2005a,b) pointed out that the current National Oceanographic and Atmospheric Administration (NOAA) Niño-3.4 SSTA–based definition identifies ''El Niño'' for several years that have not commonly been considered as such. They also showed that the composite average global seasonal weather anomalies associated with these so-called date line El Niño years are substantially different from those averaged over those more commonly agreed upon as El Niño years (called ''conventional El Niño'' years by Larkin and Harrison). This suggests a need for distinguishing some years with warm tropical Pacific SSTA from others for the purposes of seasonal climate monitoring and prediction. A methodology for doing this, however, was not suggested by Larkin and Harrison. Since then, a number of studies have focused on the characteristics of periods with tropical Pacific SST anomalies of substantial magnitude but with spatial distribution distinct from the conventional El Niño years (e.g., Ashok et al. 2007; Weng et al. 2007; Wang and Hendon 2007; Kug et al. 2009). An index for this other

type of variability has been suggested by Ashok et al. (referred to as ''El Niño Modoki'' in this case); however, we are not aware of substantial attempts since then to refine the determination methods for the conventional events, and the perspective offered by the OLR index mainly considered here cannot be recovered from the currently published lists of El Niño Modoki years [e.g., Ashok et al. list December–February (DJF) periods from two of the years distinguished by OLR—1986/87 and 1991/92—along with several other years not particularly distinguished by OLR—1979/80, 1991/92, 1992/93, 1994/95, 2002/03, and 2004/05—as El Niño Modoki years]. Thus, there remains a need to distinguish the ''conventional'' El Niño events in a way that preserves the previously documented relationships between warm-ENSO variability and global weather anomalies that have become useful outside of the scientific literature. Because the teleconnections involved in allowing the weather anomalies to persist are driven by anomalous atmospheric heating caused by changes in tropical Pacific convection conditions, and OLR anomalies are more closely related to these conditions than SST or SLP, using OLR information to do this likely offers advantages over using just surface marine variables. Because the years distinguished by the eastern-central Pacific OLR index are commonly identified as El Niño years for these purposes (e.g., Hoerling and Ting 1994; Ropelewski and Halpert 1996; Kumar and Hoerling 1997; Mason and Goddard 2001; Smith and O'Brien 2001; Patten et al. 2003; Enloe et al. 2004; Smith et al. 2007), we suggest eastern-central Pacific OLR information can fulfill this need.

It remains to confirm that significant and robust seasonal weather anomalies occur in the years distinguished by OLR. Although the relatively few number of years in this case likely limits the overall statistical significance that can be placed on composite averages, we plan to pursue this in future work.

From an OLR-based perspective, it is clear that the events of 1982/83, 1986/87, 1991/92, and 1997/98 deserve special recognition. We believe it makes good sense to distinguish these events from others in the satellite era that have been related to warm-ENSO by some indices (i.e., 1994/95, 2002/03, 2004/05, and 2006/07) but do not show convection over the eastern-central Pacific. The variability of the tropical Pacific in the years not distinguished by the OLR index proposed here is intrinsically interesting, and a better understanding of the factors that can push or limit the variability into one of these classes is needed. Unfortunately, the limited number of events observed in the satellite era prohibits a rigorous comparison of the mechanisms that control this, though this is likely fertile ground for future studies.

TABLE 3. Index standard deviation σ and DOF yr^{-1} for January 1979–December 2007. All anomalies are relative to a 1979–2007 base period, and SST information is from the ERSST dataset. Filtered versions are those discussed in text; 3-month running average for SSTA and 13-month weighted filter suggested by Trenberth (1984) for SOI. Note that the sometimes used multiplicative factor of 10 is not applied to SOI in this case.

	σ (monthly values)	σ (filtered values)	DOF yr^{-1}
ECP OLRA	11.4 W m^{-2}	n/a	1
CA92 OLRA	14.05 W m^{-2}	n/a	1
ESPI	0.9285	n/a	1
SOI	0.82	0.59	1
Niño-4	0.61°C	0.59°C	1
Niño-3.4	0.86°C	0.84°C	1
Niño-3	0.93°C	0.90°C	1
Niño-1+2	1.17°C	1.12°C	1

Acknowledgments. This manuscript benefited from comments from K. Trenberth, N. Bond, and three anonymous reviewers. This publication is (partially) funded by the Joint Institute for the Study of the Atmosphere and Ocean (JISAO) under NOAA Cooperative Agreement NA17RJ1232.

APPENDIX

Gaussian Distribution Confidence Intervals

To aid comparison of the distributions of monthly averages discussed earlier, we compare observed results to those expected from a commensurate Gaussian-distributed variable (see hash marks in Fig. 6). Here we describe how the most probable value, the 5% confidence interval, and the 95% confidence interval were determined. In this case, the 95% level corresponds to the value that a Gaussian-distributed variable, with a mean and σ equivalent to observations, would exceed, on average, in only 1 of 20 chances, based on random selection (likewise, the chance of not reaching the 5% level is 1 in 20).

We first determine σ and the degrees of freedom contained in each time series (values shown in Table 3). Degrees-of-freedom values used here are determined by estimating the time between independent samples based on the time lags at which the lagged autocorrelation of each index crosses 0. Trials have shown that the results shown in Fig. 6 are not highly sensitive to the degrees of freedom specified (e.g., qualitatively similar results are obtained when using 1–3 degrees of freedom per year).

Then we generated multiple hypothetical time series using a Gaussian random-number generator (this was

done using MATLAB's ''Randn'' function). We select hypothetical time series from a Gaussian distribution with a mean and standard deviation equivalent to observations. The number of values in each hypothetical time series was set to the number of degrees of freedom contained in the monthly averaged observations, during the 1979–2007 period discussed here (348 months in all). A library of 100 000 hypothetical time series was generated for each case.

Each member of this library was then binned according to the procedure used for the observations. The bin values were then sorted in rank order from 1 to 100 000. The average number of values in each bin determines the expected value (middle hash in Fig. 6). The 5000th value determines the 5% level and the 95 000th determines the 95% level. Experiment has shown that these levels are stable over multiple repetitions of this procedure relative to the differences seen between observational results.

REFERENCES

Arkin, P. A., and B. N. Meisner, 1987: The relationship between large-scale convective rainfall and cold cloud over the Western Hemisphere during 1982–1984. *Mon. Wea. Rev.,* **115,** 51–74.

Ashok, K., S. K. Behera, S. A. Rao, H. Weng, and T. Yamagata, 2007: El Niño Modoki and its possible teleconnection. *J. Geophys. Res.,* **112,** C11007, doi:10.1029/2006JC003798.

Barnston, A. G., M. Chelliah, and S. B. Goldberg, 1997: Documentation of a highly ENSO-related SST region in the equatorial Pacific. *Atmos.–Ocean,* **35,** 367–383.

Bretherton, C. S., C. Smith, and J. M. Wallace, 1992: An intercomparison of methods for finding coupled patterns in climate data. *J. Climate,* **5,** 541–560.

Chelliah, M., and P. Arkin, 1992: Large-scale interannual variability of monthly outgoing longwave radiation anomalies over the global tropics. *J. Climate,* **5,** 371–389.

Chiodi, A. M., and D. E. Harrison, 2008: Characterizing the interannual variability of the equatorial Pacific: An OLR perspective. NOAA Tech. Memo. OAR PMEL-140 (NTIS PB2008-112890), 30 pp.

Curtis, S., and R. Adler, 2000: ENSO indices based on patterns of satellite-derived precipitation. *J. Climate,* **13,** 2786–2793.

Deser, C., and J. M. Wallace, 1987: El Niño events and their relationship to the Southern Oscillation: 1925–1986. *J. Geophys. Res.,* **92** (C13), 14 189–14 196.

Enloe, J., J. J. O'Brien, and S. R. Smith, 2004: ENSO impacts on peak wind gusts in the United States. *J. Climate,* **17,** 1728–1737.

Garreaud, R. D., and J. M. Wallace, 1997: The diurnal march of convective cloudiness over the Americas. *Mon. Wea. Rev.,* **125,** 3157–3171.

——, and ——, 1998: Summertime incursions of midlatitude air into subtropical and tropical South America. *Mon. Wea. Rev.,* **126,** 2713–2733.

Harrison, D. E., and N. K. Larkin, 1997: The Darwin sea level pressure record, 1876–1996: Evidence for climate change? *Geophys. Res. Lett.,* **24,** 1779–1782.

——, and ——, 1998: El Niño-Southern Oscillation sea surface temperature and wind anomalies, 1946–1993. *Rev. Geophys.,* **36,** 353–399.

Hoerling, M. P., and M. Ting, 1994: On the organization of extratropical transients during El Niño. *J. Climate,* **7,** 745–766.

Kug, J.-S., F.-F. Jin, and S.-I. An, 2009: Two types of El Niño events: Cold tongue El Niño and warm pool El Niño. *J. Climate,* **22,** 1499–1515.

Kumar, A., and M. P. Hoerling, 1997: Interpretation and implications of observed inter–El Niño variability. *J. Climate,* **10,** 83–91.

Larkin, N. K., and D. E. Harrison, 2005a: Global seasonal temperature and precipitation anomalies during El Niño autumn and winter. *Geophys. Res. Lett.,* **32,** L16705, doi:10.1029/2005GL022860.

——, and ——, 2005b: On the definition of El Niño and associated seasonal average U.S. weather anomalies. *Geophys. Res. Lett.,* **32,** L13705, doi:10.1029/2005GL022738.

Lau, K.-M., H.-T. Wu, and S. Bony, 1997: The role of large-scale atmospheric circulation in the relationship between tropical convection and sea surface temperature. *J. Climate,* **10,** 381–392.

Leetmaa, A., W. Higgins, D. Anderson, P. Delecluse, and M. Latif, 2001: Application of seasonal to interannual predictions: A Northern Hemisphere perspective. *Observing the Oceans in the 21st Century,* C. J. Koblinsky and N. R. Smith, Eds., Bureau of Meteorology, 39–47.

Leith, C. E., 1973: The standard error of time-averaged estimates of climatic means. *J. Appl. Meteor.,* **12,** 1066–1069.

Liebmann, B., and C. A. Smith, 1996: Description of a complete (interpolated) outgoing longwave radiation dataset. *Bull. Amer. Meteor. Soc.,* **77,** 1275–1277.

Mason, S. J., and L. Goddard, 2001: Probabilistic precipitation anomalies associated with ENSO. *Bull. Amer. Meteor. Soc.,* **82,** 619–638.

Patten, J. M., S. R. Smith, and J. J. O'Brien, 2003: Impacts of ENSO on snowfall frequencies in the United States. *Wea. Forecasting,* **18,** 965–980.

Rasmusson, E. M., and T. H. Carpenter, 1982: Variations in tropical sea surface temperature and surface wind fields associated with the Southern Oscillation/El Niño. *Mon. Weather Rev.,* **110,** 354–384.

Ropelewski, C. F., and M. S. Halpert, 1987: Global and regional scale precipitation patterns associated with the El Niño/Southern Oscillation. *Mon. Wea. Rev.,* **115,** 1606–1626.

——, and ——, 1996: Quantifying Southern Oscillation–precipitation relationships. *J. Climate,* **9,** 1043–1059.

Smith, S. R., and J. J. O'Brien, 2001: Regional snowfall distributions associated with ENSO: Implications for seasonal forecasting. *Bull. Amer. Meteor. Soc.,* **82,** 1179–1191.

——, D. M. Legler, M. J. Remigio, and J. J. O'Brien, 1999: Comparison of 1997–98 U.S. temperature and precipitation anomalies to historical ENSO warm phases. *J. Climate,* **12,** 3507–3515.

——, C. Tartaglione, J. J. O'Brien, and J. Brolley, 2007: ENSO's impact on regional U.S. hurricane activity. *J. Climate,* **20,** 1404–1414.

Trenberth, K. E., 1984: Signal versus noise in the Southern Oscillation. *Mon. Wea. Rev.,* **112,** 326–332.

——, 1997: The definition of El Niño. *Bull. Amer. Meteor. Soc.,* **78,** 2771–2777.

——, and J. M. Caron, 2000: The Southern Oscillation revisited: Sea level pressures, surface temperatures, and precipitation. *J. Climate,* **13,** 4358–4365.

——, G. W. Branstator, D. Karoly, A. Kumar, N.-C. Lau, and C. Ropelewski, 1998: Progress during TOGA in understanding and modeling global teleconnections associated with tropical sea surface temperatures. *J. Geophys. Res.,* **103,** 14 291–14 324.

Waliser, D. E., and W. F. Zhou, 1997: Removing satellite equatorial crossing time biases from the OLR and HRC datasets. *J. Climate,* **10,** 2125–2146.

Wang, G., and H. H. Hendon, 2007: Sensitivity of Australian rainfall to inter–El Niño variations. *J. Climate,* **20,** 4211–4226.

Weng, H., K. Ashok, S. K. Behera, S. A. Rao, and T. Yamagata, 2007: Impacts of recent El Niño Modoki on dry/wet conditions in the Pacific rim during boreal summer. *Climate Dyn.,* **29,** 113–129.

Wilks, D. S., 1995: *Statistical Methods in the Atmospheric Sciences—An Introduction*. International Geophysics Series, Vol. 59, Academic Press, 467 pp.

——, 2006: On ''field significance'' and the false discovery rate. *J. Appl. Meteor. Climatol.,* **45,** 1181–1189.

Wolter, K., and M. S. Timlin, 1998: Measuring the strength of ENSO events: How does 1997/98 rank? *Weather,* **53,** 315–324.

Wyrtki, K., 1975: El Niño—The dynamic response of the equatorial Pacific Ocean to atmospheric forcing. *J. Phys. Oceanogr.,* **5,** 572–584.